

Atomic Structure of the GaAs(001)-(2 × 4) Surface Resolved Using Scanning Tunneling Microscopy and First-Principles Theory

V. P. LaBella, H. Yang, D. W. Bullock, and P. M. Thibado

Department of Physics, The University of Arkansas, Fayetteville, Arkansas 72701

Peter Kratzer and Matthias Scheffler

Fritz-Haber-Institut der Max-Planck-Gesellschaft, Faradayweg 4-6, D-14195 Berlin (Dahlem), Germany

(Received 11 February 1999)

The atomic arrangement of the technologically important As-rich GaAs(001)-(2 × 4) reconstructed surface is determined using bias-dependent scanning tunneling microscopy (STM) and first-principles electronic structure calculations. The STM images reveal the relative position and depth of the atomic-scale features within the trenches between the top-layer As dimers, which are in agreement with the $\beta_2(2 \times 4)$ structural model. The bias-dependent simulated STM images reveal that a retraction of the topmost dangling bond orbitals is the novel electronic mechanism that enables the STM tip to image the trench structure.

PACS numbers: 68.35.Bs, 61.16.Ch, 61.50.Ah, 81.05.Ea

The most technologically important surface within the family of zinc-blende III-V semiconductors is the As-rich GaAs(001)-(2 × 4) surface [1–4]. Consequently, over the past decade, state-of-the-art techniques from both theory and experiment have focused on uncovering the atomic structure of this surface [5–16]. The γ , β , β_2 , and α are four different structural models for the GaAs(001)-(2 × 4) surface, which have been extensively debated over the past decade, and are shown in Figs. 1(a)–1(d), respectively. Intensity differences in the fractional order spots in the reflection high-energy electron diffraction (RHEED) patterns were used to identify the structure of three 2 × 4 phases: γ , β , and α , prepared under different growth conditions [9]. However, changes in RHEED spot intensities may also arise from disorder rather than a periodic structural change in the unit cell. This motivated local real-space scanning tunneling microscopy (STM) experiments of differently prepared GaAs(001)-(2 × 4) surfaces, which observed structures consistent with both two and three As-dimer models [8,10,12]. More recently, STM experiments of these three phases suggest that they all have the same unit cell structure, one with two top-layer As dimers, such as the α or β_2 [13,14]. Theoretical modeling concluded that the α and β_2 structures have the lowest formation energy and the $c(2 \times 8)$ variety of the β_2 structure is the most favorable [5,11,16].

The above studies demonstrate that disorder inhibits an accurate determination of what is ideally sought, the surface structure with the lowest energy. Consequently, *in situ* grazing incidence x-ray diffraction measurements were carried out on a well-ordered GaAs(001)-(2 × 4) surface and observed a structure that is in agreement with the β_2 model [15]. Complimentary to x-ray studies would be a STM study of the local real-space atomic structure. However, to date, the structure between the

top-layer As-dimer rows, i.e., within the trenches of the GaAs(001)-(2 × 4) surface, has not been resolved. This may be due to either geometric sample-tip convolution effects (i.e., a dull tip) [17] or a negligible number of states available for tunneling at typical imaging biases [18,19].

In this Letter, the atomic structure of the As-rich GaAs(001)-(2 × 4) surface reconstruction is determined using STM and first-principles electronic-structure calculations. Comparing filled-state bias-dependent images from both theory and experiment reveals that the top-layer As dangling bond orbitals retract, allowing the finite size STM tip to image the structure in between. This is a novel mechanism that is different from a geometric tip-sample convolution effect or a change in the local density of states (LDOS) of the imaged features within trenches.

Experiments were carried out in an ultrahigh vacuum (UHV) multichamber facility [(5–8) × 10⁻¹¹ Torr throughout] which contains a molecular beam epitaxy (MBE) chamber (Riber 32P) that includes a substrate temperature determination system accurate to ±2 °C [20]. This chamber is connected to a surface analysis chamber,

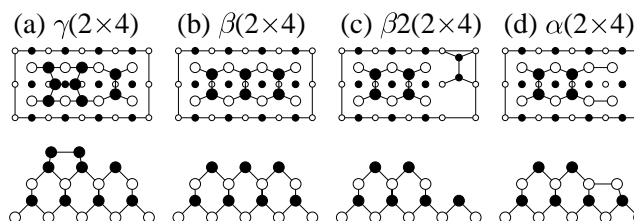


FIG. 1. Four proposed structural models of the GaAs(001)-(2 × 4) surface reconstruction. Each model shows two views, top (above) and side (below), and the names given to the structural model is indicated in the figure. Filled and empty circles represent As and Ga, respectively. Larger circles represent atoms closer to the surface.

which contains an Omicron STM [21]. Commercially available, “epi-ready,” $n+$ (Si-doped $10^{18}/\text{cm}^3$) GaAs(001) $\pm 0.1^\circ$ substrates were loaded into the MBE system without any chemical cleaning. The surface oxide layer was removed and a $1.5\text{-}\mu\text{m}$ -thick GaAs buffer layer was grown at 580°C using a growth rate of $1.0\ \mu\text{m}/\text{h}$ as determined by RHEED oscillations and an As_4 to Ga beam equivalent pressure (BEP) ratio of 15. Motivated by the desire to achieve a well-ordered surface the following algorithm was developed using feedback from both RHEED and *in situ* STM. The substrate was annealed at 600°C with an As_4 BEP of $1.0\ \mu\text{Torr}$ for 15 min and then at 570°C with the same As_4 BEP for an additional 15 min [22]. After this, the sample was cooled to 450°C at a rate of $1.5^\circ\text{C}/\text{s}$ while simultaneously ramping the As_4 BEP to zero by the time the sample reached 500°C . The sample was held at 450°C for 15 min to allow the As_4 to be pumped out of the chamber [23,24]. Finally, the sample was cooled at a rate of $1.5^\circ\text{C}/\text{s}$ to room temperature, transferred to the STM without breaking UHV, and imaged at room temperature.

The large-scale STM images showed a nearly defect-free surface with $\sim 1\text{-}\mu\text{m}$ -wide terraces, consistent with the sharp (2×4) -RHEED pattern. Numerous small-scale STM images were acquired from the same region using filled-state sample biases ranging from -3.0 to -2.1 V in 0.1 V increments and a constant tunneling current ($0.01\text{--}0.50$ nA). The STM tips were manufactured from single-crystal, $\langle 111 \rangle$ -oriented tungsten wire that was electrochemically etched under high magnification ($\sim 1000\times$) and electron-beam heated *in situ* to remove any oxide.

Simulated STM images were extracted from density functional calculations without modeling the STM tip [3,25]. These calculations were performed within the local-density approximation by employing a plane-wave pseudopotential approach with a cutoff energy of 10 Ryd [26]. The GaAs(001) surface was modeled as a seven-layer slab followed by a vacuum region larger than 2 nm. The bottom layer of atoms was passivated with pseudohydrogen atoms and kept fixed, while the top six layers were relaxed until all the forces were less than 0.5 eV/nm. After structural relaxation, extracting isocontour surfaces of a suitably defined local density of states generated numerically simulated constant current STM images. The local density of valence band states were integrated from the valence band minimum (VBM) to 0.3 and 1.1 eV below the VBM. This mimics the range of the filled-state sample biases used in the STM images, which are referenced with respect to the Fermi level of the sample located in the middle of the 1.4 eV surface band gap [27].

A filled-state STM image ($11\ \text{nm} \times 11\ \text{nm}$) taken with a sample bias of -2.1 V is shown in Fig. 2(a). The multiple bright rows, running diagonally across the image, have a center-to-center distance of 1.6 nm along the

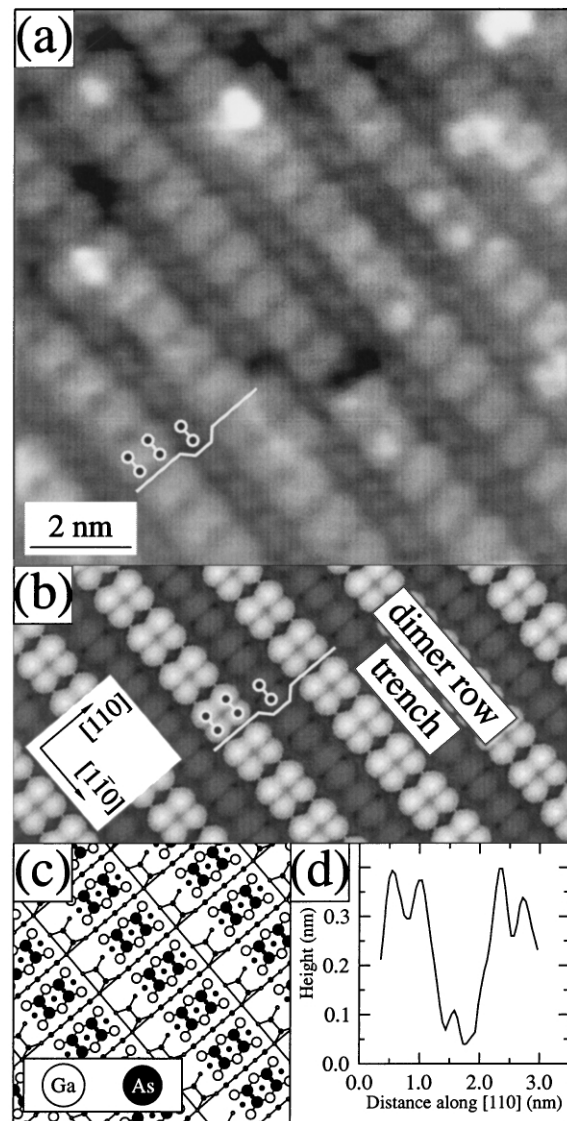


FIG. 2. (a) Filled-state STM image acquired with a sample bias of -2.1 V measuring $11\ \text{nm} \times 11\ \text{nm}$, (b) simulated STM image of the β_2 structural model using a filled-state bias of 0.3 V below the valence band maximum, (c) β_2 structural model, and (d) height cross section across a dimer trench along the $[110]$ direction extracted from the STM image shown in (a).

$[110]$ direction, representing the “4-by” periodicity of the (2×4) reconstruction. Along the $[1\bar{1}0]$ direction another oscillation in the gray level occurs at twice the spatial frequency or every 0.8 nm, representing the “2-by” periodicity of the (2×4) reconstruction. These 2-by features are topographically flat and have an overall width of ~ 0.9 nm along the $[110]$ direction. These features indicate that the top-layer structure consists of two dimers of equal height as depicted by the two ball-and-stick dimer models drawn over the STM image in Fig. 2(a). This is inconsistent with the γ model [cf. Fig. 1(a)] which would have an additional As dimer on top of the row. It is also inconsistent with the β model

[cf. Fig. 1(b)] which would have a feature spanning over three-fourths of the length of the 4-by width.

The structure within the trenches between the top-layer As-dimer rows is also resolved in Fig. 2(a). The periodicity of the trench structure is 0.8 nm along the $[1\bar{1}0]$ direction, similar to the 2-by periodicity of the top-layer dimer rows. However, this trench periodicity is shifted out of phase with the 2-by periodicity of the top-layer dimer rows, indicated by the white line and the three ball-and-stick As dimers drawn over the data. This shift is inconsistent with the α model, which has a symmetric arrangement of atomic features between the trenches and the top layer [cf. Fig. 1(c)]. This shift and all of the other observed features in Fig. 2(a) are in agreement with the $\beta 2$ model [cf. Fig. 1(d)].

A first-principles-generated STM image of the $\beta 2(2 \times 4)$ structural model at a filled-state bias of 0.3 V below the VBM is displayed in Fig. 2(b) as a continuation of the STM data shown in Fig. 2(a). The simulated STM data assumes an infinitely sharp STM tip, providing more resolution than obtained experimentally. Nevertheless, excellent agreement between the two images is achieved. Namely, the width of the top-layer 2-by features along the $[110]$ direction is reproduced. In addition, the relative shift between the top-layer 2-by features and the 2-by features within the trenches is reproduced. This is indicated with the white line and the three ball-and-stick As dimers drawn over the simulated image. This point-by-point two-dimensional comparison of first-principles theory and STM data indicates, in exhaustive detail, that the imaged surface has the same structure as the $\beta 2$ model. For clarity, a ball-and-stick $\beta 2$ structural model is drawn to scale in Fig. 2(c) as a continuation of Fig. 2(b).

A height cross section taken along the $[110]$ direction from the STM data displayed in Fig. 2(a) is shown as a line scan in Fig. 2(d). This height cross section spans two top-layer dimer rows and the trench between them. This line scan shows that the topographic depth change that occurs between the dimer rows is ~ 0.3 nm, or a full monolayer (ML) height for GaAs(001) [28]. This is in agreement with the $\beta 2$ model [cf. Fig. 1(c)] and in disagreement with the α model, which would show a height difference of only half a monolayer (0.14 nm) [cf. Fig. 1(d)].

The filled-state STM images taken at a typical GaAs(001) sample bias of -3.0 V did not reveal the structure of the surface within the trenches. A $2.8 \text{ nm} \times 4.4 \text{ nm}$ section of this image is shown in Fig. 3(a). However, the internal structure of the top-layer 2-by features is better resolved at these larger biases. Namely, a distinct single minimum exists at the center of the top-layer dimer row, indicating the presence of only two As dimers in the top layer and further supporting the $\beta 2$ model. This single minimum is less pronounced in the image taken of the same region but

with a smaller sample bias of -2.1 V shown in Fig. 3(b). Most significantly, this smaller-bias STM image reveals the atomic structure within the trenches. This structure first appeared in the series of images at -2.6 V and its intensity was monotonically increased as the bias was lowered to -2.1 V.

A bias-dependent feature in a STM image typically results from variations in the local density of states of the bias-dependent feature [18]. Interestingly, LDOS calculations for the As dimers in the trench reveal that there are a nearly uniform number of states available for tunneling at all filled-state biases starting from the VBM. This rules out a change in the trench dimer's LDOS as a possible explanation for the observed bias dependence.

The mechanism that explains this bias-dependent difference in the STM images was discovered after bias-dependent simulated STM images were produced. The simulated STM images taken at filled-state biases of 1.1 and 0.3 V below the VBM are shown rendered in three dimensions in Figs. 3(c) and 3(d), respectively. These images reveal a mammoth 0.3 nm increase in the physical width of the trench region as the filled-state bias is reduced by 0.8 V. This increase is monotonic, and is consistent with the monotonic change in the bias-dependent STM images. The trench widens as a result of the retracting surface of constant LDOS about the top-layer As-dimer dangling bond orbital. This retraction allows the STM tip to penetrate between the top-layer As-dimer rows and image the As dimers within the trenches that are a monolayer (0.28 nm) lower. At larger biases, the narrower trench

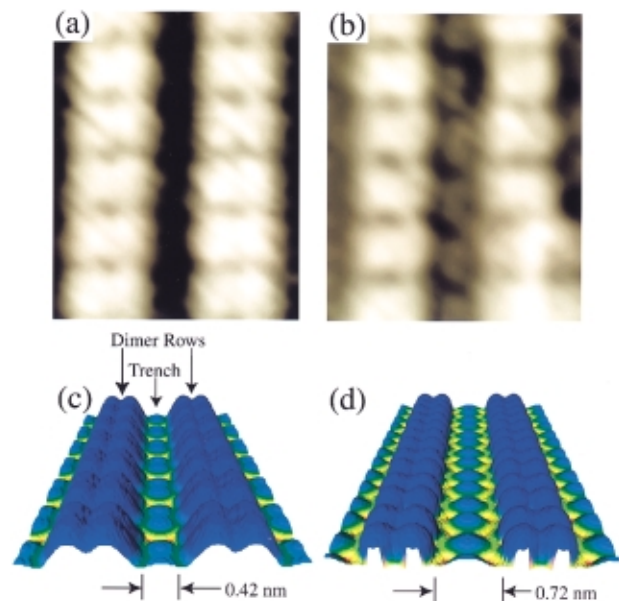


FIG. 3 (color). (a),(b) $2.8 \text{ nm} \times 4.4 \text{ nm}$ filled-state STM images of the same area acquired with sample biases of -3.0 and -2.1 V, respectively. (c),(d) Simulated STM images using filled-state biases of 1.1 and 0.3 V below the valence band maximum, respectively.

results in the tunneling current jumping from one top-layer As dimer to the next, missing the features in between. Thus, even though the As dimers within the trench have a uniform LDOS, at high biases those states are blocked by the orbitals of the top-layer As dimers.

An apt analogy for explaining the inability to image features within the trenches at larger biases is a geometric sample-tip convolution effect commonly seen in scanning probe microscopy [17]. However, geometric convolution effects do not disappear as the bias is lowered. In addition, they typically happen on length scales which are at least an order of magnitude or more larger than the 0.3 nm observed here. This new phenomenon can be described as an electronic sample-tip convolution effect. In this phenomenon, the step edge of the trench is sharper at smaller biases, and this electronic sample sharpening reduces the geometric tip-sample convolution, allowing the finite size tip to image inside the trench. This is a novel contrast mechanism that helps bring to a close the decade-long search for the atomic structure of the well-ordered technologically important GaAs(001)-(2 × 4) reconstructed surface. In addition, it may help in obtaining accurate structural models for other important surface reconstructions. Another interesting consequence of this tunable trench width is that it brackets the area of the tunneling region of the STM tip. When the trench width is 0.42 nm the tip cannot image the third layer, while it can when the width is 0.72 nm. This information provides a significant constraint to the ongoing investigations concerning the spatial extent of the tunneling current and its effects on the resolution of the STM [19,29–31].

In conclusion, this Letter presents the first STM images that resolve all the atomic features associated with the GaAs(001)-(2 × 4) reconstructed surface. The bias-dependent experimental and first-principles-generated images agree on several features that conclusively point to the $\beta 2$ model as the correct structural model for the well-ordered GaAs(001)-(2 × 4) reconstructed surface. The clear understanding of the imaged features, especially the bias-dependent ones, would not have been possible without the comparison to first-principles calculations. The theory and data show that the dimer trench widens as the filled-state bias is reduced. It is believed that this novel, purely electronic-based, widening of the trench region is what allows the STM tip to image the structure within. To our knowledge, this is the first time this type of electronic tip-sample convolution effect has been reported. Furthermore, it is the first time subsurface features have been theoretically modeled, potentially providing insight into other subsurface STM measurements. In addition, the ex-

cellent agreement between first-principles theory and STM data in reproducing both the electronic and geometric features further advances the state-of-the-art in both areas and emphasizes the need for both in determining atomic surface structure.

We are grateful to L. Bellaiche for critical reading of this manuscript, and to G. Schwarz and S. Erwin for their helpful comments. This work was supported in part by the Office of Naval Research Grant No. N00014-97-1-1058 and the National Science Foundation Grant No. DMR-9733994.

-
- [1] A. Kley *et al.*, Phys. Rev. Lett. **79**, 5278 (1997).
 - [2] M. Itoh *et al.*, Phys. Rev. Lett. **81**, 633 (1998).
 - [3] P. M. Thibado *et al.*, Phys. Rev. B **53**, R10481 (1996).
 - [4] See, for example, special issue of Compound Semicond. **4**(6) (1998).
 - [5] D. J. Chadi, J. Vac. Sci. Technol. A **5**, 834 (1987).
 - [6] H. H. Farrell *et al.*, J. Vac. Sci. Technol. B **5**, 1482 (1987).
 - [7] M. D. Pashley *et al.*, Phys. Rev. Lett. **60**, 2176 (1988).
 - [8] G.-X. Qian *et al.*, Phys. Rev. B **38**, 7649 (1988).
 - [9] H. H. Farrell *et al.*, J. Vac. Sci. Technol. B **8**, 903 (1990).
 - [10] D. K. Biegelsen *et al.*, Phys. Rev. B **41**, 5701 (1990).
 - [11] J. E. Northrup *et al.*, Phys. Rev. B **50**, 2015 (1994).
 - [12] L. Broekman *et al.*, Surf. Sci. **331–333**, 1115 (1995).
 - [13] T. Hashizume *et al.*, Phys. Rev. B **51**, 4200 (1995).
 - [14] A. R. Avery *et al.*, Phys. Rev. Lett. **76**, 3344 (1996).
 - [15] Y. Garreau *et al.*, Phys. Rev. B **54**, 17638 (1996).
 - [16] N. Moll *et al.*, Phys. Rev. B **54**, 8844 (1996).
 - [17] R. Wiesendanger, *Scanning Probe Microscopy and Spectroscopy, Methods and Applications* (Cambridge University Press, Cambridge, England, 1994), p. 100.
 - [18] R. M. Feenstra *et al.*, Phys. Rev. Lett. **58**, 1192 (1987).
 - [19] J. A. Kubby *et al.*, Surf. Sci. Rep. **26**, 61 (1996).
 - [20] P. M. Thibado *et al.*, J. Vac. Sci. Technol. B **17**, 253 (1999).
 - [21] J. B. Smathers *et al.*, J. Vac. Sci. Technol. B **16**, 3112 (1998).
 - [22] In our system at an As₄ BEP of 1.0 μTorr and a substrate temperature of 425 °C, the GaAs(001) (2 × 4)-to-c(4 × 4) surface phase transition is observed.
 - [23] M. D. Johnson *et al.*, Surf. Sci. **298**, 392 (1993).
 - [24] H. Yang *et al.*, J. Cryst. Growth **201–202**, 88 (1999).
 - [25] S. Heinze *et al.*, Phys. Rev. B **58**, 16432 (1998).
 - [26] M. Bockstedte *et al.*, Comput. Phys. Commun. **107**, 187 (1997).
 - [27] M. D. Pashley *et al.*, Phys. Rev. B **48**, 4612 (1993).
 - [28] A ML of GaAs is 0.28 nm high, composed of a plane of both Ga and As, and sometimes referred to as a bilayer.
 - [29] N. D. Lang *et al.*, Phys. Rev. Lett. **63**, 1499 (1989).
 - [30] J. Tersoff, Phys. Rev. B **39**, 1052 (1989).
 - [31] H. Sirringhaus *et al.*, Phys. Rev. Lett. **74**, 3999 (1995).